Atmos. Chem. Phys. Discuss., 9, 5753–5783, 2009
www.atmos-chem-phys-discuss.net/9/5753/2009/

Atmospheric Chemistry and Physics Discussions

This discussion paper is/has been under review for the journal *Atmospheric Chemistry and Physics (ACP)*. Please refer to the corresponding final paper in *ACP* if available.

Retrieval of water vapor profile in the mesosphere from satellite ozone and hydroxyl measurements by the basic dynamic model of mesospheric photochemical system

M. Yu. Kulikov[1], **A. M. Feigin**[1], **and G. R. Sonnemann**[2]

[1]Institute of Applied Physics of the Russian Academy of Science, Ulyanov Str. 46, 603950, Nizhny Novgorod, Russia
[2]Leibniz-Institute of Atmospheric Physics at the University Rostock in Kühlungsborn, Schloss-Str. 6, 18225 Ostseebad Kühlungsborn, Germany

Received: 9 December 2008 – Accepted: 28 January 2009 – Published: 4 March 2009

Correspondence to: M. Yu. Kulikov (kulm@appl.sci-nnov.ru)

Published by Copernicus Publications on behalf of the European Geosciences Union.

Abstract

We propose an indirect method for retrieving a number of significant minor gas constituents of the atmosphere. The technique is based on the use of so-called basic dynamic models of atmospheric photochemical systems simplified mathematically correctly in a special manner. It is applied to a mesospheric system describing day evolution of key minor gas constituents at these heights. We take as initial data experimental data of the CRISTA-MAHRSI satellite campaign of August 1997 during which ozone and hydroxyl (O_3 and OH) concentrations were measured simultaneously. It is demonstrated that the use of the basic dynamic model allows retrieval of vertical distribution (within the 53–85 km range of heights) of water vapor concentration that is one of the control parameters of the mesospheric photochemistry.

1 Introduction

Observation of minor gas constituents (MGC) is traditionally one of the fundamental problems in investigations of the Earth's atmosphere. MGC evolution is controlled by photochemical processes which, being one of the basic sources of air heating in the middle atmosphere, influence the majority of atmospheric parameters and govern one of the key mechanisms of anthropogenic action on processes in an atmosphere.

As the number of MGCs that can be measured directly and regularly is still rather scanty, indirect methods are a useful tool. They are based on using a priori knowledge about possible relationship between measured and inferred characteristics and allow obtaining additional information about the most significant atmospheric MGCs from available experimental data. Mathematical models of photochemical systems (equations of chemical kinetics for MGC concentrations involving transport processes) may be regarded to be the main candidates for a "supplier" of a priori relationships. These models have been developed and verified for most regions of the Earth's atmosphere. However, high dimension hinders wide application of these models for obtaining in-

ACPD

9, 5753–5783, 2009

formation about concentrations on non-measured and/or unmeasurable MGCs. Atmospheric photochemical systems (APCS) contain, as a rule, several tens and more chemical constituents reacting with each other and evolution of these systems depends on a large amount of parameters. In this work we propose a method for retrieving atmospheric MGC concentrations that are not measured directly. The method is based on using mathematically correctly simplified APCS models referred to, following the work by Feigin and Konovalov (1996), as basic dynamic models (BDM). BDMs retain, within the considered region of the parameter values, basic qualitative and quantitative properties of a "complete" system and include a minimum possible number of dynamic variables described by differential equations. The key idea of constructing such models is to divide variables of the system (concentrations of chemical constituents) into two groups according to the relationship between characteristic time of their evolution, "τ", and time scale of the studied phenomenon, τ_0. Variables of the first group are "fast": $\tau \ll \tau_0$. Taking into consideration dissipativity of APCS, they are supposed to be in the state of instantaneous stable equilibrium. Their "instantaneously equilibrium" values are determined from a system of algebraic equations obtained by equating to zero time derivatives in the corresponding equations of chemical kinetics of the initial (complete) system. These values are generally functions of parameters and of the slow (dynamic) variables referred to the second group whose evolution with characteristic time $\tau \approx \tau_0$ is described by differential equations. Thus, the procedure of BDM construction allows one to find asymptotically correctly a maximum possible number of algebraic relationships between constituents of the considered photochemical system. It is quite apparent that these relationships are the most convenient tool for inferring from available data of experiments information about significant MGCs of the atmosphere. In addition, if all dynamic variables of the BDM are inferred from algebraic equations, there arises a possibility to use a system of BDM differential equations for seeking values of the most important ("control") parameters determining the evolution of MGC concentrations.

In this work the above approach is applied to a mesospheric photochemical system

ACPD
9, 5753–5783, 2009

(MPCS) that describes evolution of key MGCs (O, O(^{1}D), O_3, H, OH, HO_2) of the Earth's mesosphere (50–90 km heights). We take as initial data experimental data of the CRISTA-MAHRSI satellite campaign of August 1997 during which ozone and hydroxyl (O_3 and OH) concentrations were measured simultaneously. We demonstrate that the use of the MPCS BDM allows retrieval of vertical distribution (within the 53–85 km range of heights) of H_2O concentration that is one of the control parameters of the MPCS.

2 MPCS and the used models, general description of the method of H_2O retrieval by O_3 and OH measurements

A complete MPCS usually includes about a hundred chemical reactions with participation of more than twenty chemical constituents of the mesosphere (see e.g., Brasseur and Solomon, 1986; Fichtelmann and Sonnemann, 1989). One of the goals of this research is elucidation of the relationship between the concentrations of O_3, OH and H_2O that would allow us to retrieve vertical distribution of the latter species by vertical distribution of the two first species measured during the CRISTA-MAHRSI campaign. The complete MPCS may be reduced substantially for solution of this problem. We can consider only the chemical reactions (see Table 1) that determine evolution of the constituents of the family of odd oxygen (O, O(^{1}D), and O_3) and odd hydrogen (H, OH, and HO_2) at the heights of 50–90 km in the time interval τ_0 with a duration of approximately one day (daylight hours). From Table 1 it is clear that, first, reactions with participation of the members of the families of ClO_x and NO_x as well as with participation of CH_4, H_2, H_2O_2, and some other mesospheric MGCs weakly influence the constituents of interest to us (see Crutzen et al., 1995). Second, the key MPCS parameters governing evolution of the families of odd oxygen and hydrogen are, evidently, the temperature and concentration of air molecules. Third, in spite of the fact that photochemical reactions with participation of H_2O molecules (see Reactions R7 and R20 in Table 1) are the main source for the family of odd hydrogen, the concentration of this constituent on

ACPD
9, 5753–5783, 2009

the considered interval (daytime hours during one day) can be regarded to be constant and depending on coordinates only (e.g., Brasseur and Solomon, 1986). The latter circumstance will be used in the method of retrieval of vertical distribution of this important parameter by vertical distribution of O, $O(^1D)$, O_3, H, OH, and HO_2 that will be described below.

As was stated in Sect. 1, the proposed method is based on the BDM. The zero-dimensional BDM corresponding to the set of reactions listed in Table 1 and describing the daytime evolution of the MPCS with characteristic time scale $\tau_0 = 10^4 - 10^6$ s at the heights of 75–90 km was constructed by Feigin et al. (1998). At these heights atomic oxygen concentration has characteristic time of evolution of order τ_0, hence, it should be considered to be a slow variable. Below 75 km, the lifetime of O is markedly shorter, so its concentration at these heights should formally be regarded to be a fast variable. Nevertheless, in the MPCS BDM describing all the mesosphere in a unified manner it is correct to consider O concentration as a slow variable throughout the 50–90 km range. Concentrations of the remaining constituents ($O(^1D)$, O_3, H, OH and HO_2) are fast variables with lifetimes $<10^2$ s; here H, OH and H_2O form a slow family of odd hydrogen HO_x whose characteristic variation time is of the order of the time of variation of O concentration at the heights of 75–90 km. Thus, the zero-dimensional MPCS BDM is a system of seven equations, two of which are first-order differential equations with respect to O and HO_x concentrations:

$$\frac{d}{dt}(\mathrm{O}) = -((\mathrm{R}(1) \times M + \mathrm{R}(4)) \times \mathrm{OH} + \mathrm{R}(5) \times \mathrm{HO_2} + \mathrm{R}(9) \times \mathrm{O_2} \times M + \mathrm{R}(10) \times \mathrm{O_3} \quad (1)$$
$$+2 \times \mathrm{R}(11) \times M \times \mathrm{O}) \times \mathrm{O} + 2 \times \mathrm{R}(8) \times \mathrm{O_2} + \mathrm{R}(16) \times \mathrm{O_3}$$

$$\frac{d}{dt}(\mathrm{HO_x}) = -2 \times (\mathrm{R}(2) + \mathrm{R}(18)) \times \mathrm{H} \cdot \mathrm{HO_2} - 2 \times \mathrm{R}(3) \times \mathrm{HO_2} \times \mathrm{OH} - 2 \times \mathrm{R}(15) \quad (2)$$
$$\times \mathrm{OH}^2 - 2 \times \mathrm{R}(17) \times M \times \mathrm{OH} \times \mathrm{H} + 2 \times (\mathrm{R}(7) + \mathrm{R}(20) \times \mathrm{O}(^1D)) \times \mathrm{H_2O}$$

and the remaining equations form a system of algebraic equations that relate values of

fast variables to values of slow ("dynamic") variables and to parameters of the BDM:

$$H = HO_x - OH - HO_2 \quad (3)$$

$$HO_2 = \frac{R(6) \times O_2 \times M \times H + R(13) \times OH \times O_3}{R(5) \times O + (R(2) + R(14) + R(18)) \times H + R(3) \times OH} \quad (4)$$

$$O_3 = \frac{R(9) \times M \times O_2 \times O}{R(10) \times O + R(12) \times H + R(13) \times OH + R(16)} \quad (5)$$

$$OH = \frac{R(5) \times O \times HO_2 + R(12) \times H \times O_3 + 2 \times R(14) \times H \times HO_2}{R(4) \times O + R(13) \times O_3 + R(3) \times HO_2} \quad (6)$$

$$O(^1D) = \frac{R(16) \times O_3}{R(19) \times M} \quad (7)$$

In Eqs. (1–7), M is air concentration, R(1,...,20) are the rates of the reactions listed in Table 1; their numerical values used below correspond to the recent Jet Propulsion Laboratory data (Sander et al., 2006).

It is well known that, in the conditions of the real mesosphere, the MGC evolution is strongly affected by transport processes. For evaluation of the influence of different transport mechanisms on MGC evolution with the time scale τ_0=(10^4–10^6) s of interest to us it suffices to compare characteristic time of transport τ_{tr} and τ_0. Apparently, transport is essential, if $\tau_{tr} \leq \tau_0$. Such a comparison generally demands knowledge of the spatial scale of inhomogeneity of the studied characteristic. For the vertical distributions of MGS concentrations in the mesosphere these scales are ~(10^3–10^4) m in the vertical direction and ~10^7 m in the horizontal direction (see e.g., Brasseur and Solomon, 1986). Estimates of τ_{tr} made for known mechanisms of transport (molecular and eddy diffusion, horizontal and vertical winds, including those caused by different waves) indicate that the influence of transport on the considered MGS evolution is insignificant in the lower mesosphere (heights from 50 to 70–75 km), whereas in the

ACPD
9, 5753–5783, 2009

upper part of the modeled region (from 70–75 to 90 km) vertical eddy diffusion and transport by vertical wind should be taken into account. It is important that, according to the estimates, both these mechanisms are "slow" in the sense pointed out in Sect. 1, i.e., $\tau_{tr} \approx \tau_0$. This means that even these, most essential transport mechanisms do not break "instantaneous equilibrium" of the fast chemical constituents $O(^1D)$, O_3, H, OH, and HO_2. Their evolution is fully determined by evolution of the "slow" components O and HO_x affected by vertical diffusion and wind. In other words, concentrations of the fast components are related to concentrations of the slow components by algebraic relations (3–7) obtained within the framework of the zero-dimensional BDM throughout the modeled range of heights (50–90 km). From the said above it follows that the system of BDM MPCS differential equations must contain terms describing transport by eddy diffusion and by vertical wind:

$$\frac{\partial}{\partial t} n_i = I_i - S_i + \frac{\partial}{\partial z} D_{zz} \frac{\partial}{\partial z} n_i - \frac{\partial}{\partial z} (w_z \times n_i), \tag{8}$$

$$\{n\}_{i=1,2} = \{O, HO_x\} \tag{9}$$

Here, I_i and S_i are, respectively, photochemical sources and sinks of the concentration n_i, corresponding to the right-hand sides of Eqs. (1–2); z is height, D_{zz} stands for the coefficient of vertical eddy diffusion, and w_z is the vertical wind velocity.

In this work we employed, in addition to the MPCS BDM, two more models of mesospheric photochemistry that take into account these types of transport. First, to verify correctness of the algebraic relations (3–7) under real conditions we calculated the COMMA-IAP model (Sonnemann et al., 1998). This model describes the range of heights from 30 to 150 km and contains all reactions that are usually included in a complete MPCS. Besides, within the framework of this model all MPCS components (the fast ones included) were regarded to be dynamic variables and their evolution was determined from the corresponding differential equations. We omit description of the testing procedure and only point out that, in the 50–90 km range of heights, the algebraic system of Eqs. (3–7) describes correctly (to an accuracy not worse than 1% at

ACPD
9, 5753–5783, 2009

zenith angles of the Sun not more than 70°) the daytime relationship between $O(^1D)$, O_3, H, OH, HO_2, O, and HO_x. The algebraic system includes five equations. Note that this amount of a priori relations, with available data about simultaneous values of concentrations of two arbitrary chemical constituents of the MPCS, is quite sufficient for retrieving the values of all the other components of the system and thus for finding values of dynamic variables of the MPCS BDM (O and HO_x) and of nearly all (except terms proportional to H_2O concentration and those describing transport) terms entering into the right-hand sides of Eqs. (8–9). This important property of MPCS BDM underlies the proposed method of retrieval of H_2O concentration that uses data of O_3 and OH measurements and implies the following sequence of operations:

1. Two pairs of vertical distributions of ozone and hydroxyl $\{O_3^{in}(z), OH^{in}(z)\}$ and $\{O_3^{end}(z), OH^{end}(z)\}$ concentrations measured during one day (daylight hours) and corresponding to close values of horizontal coordinates (i.e., approximately the same values of longitude and latitude) are selected from available experimental data. The first pair of vertical distributions (morning measurements) $\{O_3^{in}(z), OH^{in}(z)\}$ must be measured at local time t_{in} before 10:00 a.m.; the second pair (evening measurements) $\{O_3^{end}(z), OH^{end}(z)\}$ must be measured at local time t_{end} after 12 o'clock in the afternoon.

2. The above data are substituted into Eqs. (3–7). After that, single-valued solutions of this system relative to unknown variables (concentrations of $O(^1D)$, H, HO_2, O, and HO_x) are found for each specified value of height $z=z_0$. As a result we determine two pairs of vertical distributions of dynamic variables of MPCS BDM $\{O^{in}(z), HO_x^{in}(z)\}$ and $\{O^{end}(z), HO_x^{end}(z)\}$ concentrations corresponding to close values of horizontal coordinates but different instants of local time t_{in} and t_{end}.

3. The obtained data and Eqs. (8–9) are used in a special procedure that enables us to retrieve unambiguously vertical distribution of H_2O concentration. This procedure is detailed in Sect. 3.

ACPD
9, 5753–5783, 2009

To test correctness of the proposed technique we took a one-dimensional (in height) complete MPCS model corresponding to the reactions listed in Table 1. Within the framework of this model, all the components (except for $O(^1D)$ concentration) were calculated as dynamic variables, with allowance for transport by vertical eddy diffusion and vertical wind. The model "supplied" conjectural data of experiments ($\{O_3^{in}(z)$, $OH^{in}(z)\}$ and $\{O_3^{end}(z)$, $OH^{end}(z)\}$) that were calculated for given distributions of water vapor concentrations $H_2O(z)$ and parameters of vertical transport. Further, we used the algorithm of retrieval of water vapor concentration described above and compared the retrieved and the "true" distribution of $H_2O(z)$. The numerical scheme for calculation of this model included 200 layers at the heights ranging from 50 to 92 km. Integration was done by Gear's BDF embedded in the Fortran PowerStation with floating time step controlled to a specified relative accuracy of 10^{-4}. The upper and lower boundary conditions for the concentrations of O_3, OH and HO_2, as well as the lower boundary conditions for the concentrations of O and H were chosen to be free: evolution of these variables at the discussed heights was determined by local (photochemical) processes and was calculated by the corresponding zero-dimensional first-order differential equations without allowance for vertical transport processes. Boundary conditions with given flows were taken as the upper boundary for O and H concentrations. Vertical wind velocity was taken in the form

$$w_z = w_0 + w_1 \times \sin(2\pi t/T_1 + \varphi_1) + w_2 \times \sin(2\pi t/T_2 + \varphi_2), \quad (10)$$

where w_0 is mean zonal velocity, $w_1, T_1, \varphi_1, w_2, T_2, \varphi_2$ are the amplitude, period and phase of vertical wind velocity in diurnal and semi-diurnal tides, respectively. Typical summer profiles from the empiric MSIS-E-90 model (Hedin, 1991) were taken as vertical distributions of temperature and air concentration. Besides, the model took into account data on real dependences of photolysis rates of water, ozone and molecular oxygen on height and local zenith angle of the Sun calculated within the framework of the COMMA-IAP model. Values of local zenith angle of the Sun as a function of local time and latitude were calculated in a standard manner.

ACPD
9, 5753–5783, 2009

3 The procedure of H_2O retrieval

Let us first analyze the case of altitudes lower than 70–75 km, where transport processes weakly affect MPCS BDM dynamics, hence, the zero-dimensional BDM of the system (1–2) is applicable. H_2O concentration at a definite height $z=z_0$ is determined by the iteration procedure started from an arbitrary initial value of concentration of the given chemical constituent. At each successive iteration step, Eqs. (1–2) are calculated within the interval of daylight local time $t \in [t_{in}, t_{end}]$ with a constant value of H_2O concentration and initial conditions $\{O^{in}=O^{in}(z_0), HO_x^{in}=HO_x^{in}(z_0)\}$, which allows finding values of dynamic variables O^{dv} and HO_x^{dv} at the time instant $t=t_{end}$. Further, the value of H_2O concentration is varied so that the subsequent calculation of the BDM evolution in the considered time interval should ensure a decreased relative difference between $\{O^{end}=O^{end}(z_0), HO_x^{end}=HO_x^{end}(z_0)\}$ and the new values of $\{O^{dv}, HO_x^{dv}\}$. The final goal of the iteration procedure is finding the value of H_2O concentration for which the error

$$S = (HO_x^{end} - HO_x{}^{dv})^2/(HO_x^{end})^2 + (O^{end} - O^{dv})^2/(O^{end})^2 \quad (11)$$

would be minimal. Our analysis demonstrates that an optimal value of H_2O concentration can be found using the simplest gradient iteration scheme

$$H_2O^{new} = H_2O^{old}(1 + \lambda \times (HO_x^{end} - HO_x{}^{dv})/HO_x^{end} + \lambda \times (O^{end} - O^{dv})/O^{end}) \quad (12)$$

Here, λ=const$\ll$1; H_2O^{old} and H_2O^{new} are, respectively, the current and subsequent values of H_2O concentration corresponding to one step of the iteration procedure. The process is finished automatically when S amounts to 10^{-8}. For verification that the found value of H_2O concentration is unique and corresponds to the global minimum of S the described procedure must be repeated for several, strongly differing initial values of H_2O concentration. These may be, for instance, values lying in the 0.1 ppmv to 100 ppmv interval that involves the range of possible values of H_2O concentrations (1–10 ppmv) in the real conditions of the mesosphere.

ACPD
9, 5753–5783, 2009

For retrieving vertical distribution of H_2O concentration above ~70–75 km one should take into account transport processes due to vertical eddy diffusion and vertical wind. Therefore, formally one should use at these heights the set of Eqs. (8–9). Analysis shows that the described above procedure using the zero-dimensional MPCS BDM may be readily generalized for a one-dimensional model, if we have a priori information about vertical distribution of vertical eddy diffusion coefficient D_{zz} and vertical wind velocity w_z. In the literature, however, values of D_{zz} at a fixed height vary in a broad interval (up to an order of magnitude or more, see e.g., Hocking, 1992) and are strongly dependent on latitude and season of the year (e.g., Danilov and Kalgin, 1992; Lübken 1993, 1997), whereas characteristics of vertical wind velocity w_z in the mesosphere have not been measured at all and numerical models or estimates based on known theoretical relations with measured characteristics of the mesosphere are, actually, the only available source of information about them. Körner and Sonnemann (2001) demonstrated that values of the mean zonal component of vertical wind velocity reach about 1–2 cm s^{-1} at 80–90 km. Characteristic amplitudes of vertical wind velocity variations in diurnal and semidiurnal tides may be found from their relationship with the amplitudes of temperature variations in these atmospheric waves. For example, for the amplitudes of temperature variations in both the tides of about 5 K typical of the summer upper mesosphere (Singer et al., 2003), the values of $w_{1,2}$ are about 5–10 cm s^{-1}.

In addition, allowance for transport in Eqs. (8–9) demands accurate calculation of the first and second derivatives of dynamic variables along the vertical coordinate, which imposes rather severe requirements on initial data of experiments. In particular, vertical resolution dz of these data must be much less than characteristic scales of variation of MPCS dynamic variables along the vertical coordinate, which may be of order 1 km or less in the upper mesosphere (e.g., Brasseur and Solomon, 1986). However, dz of almost all satellite campaigns on measuring MGCs of the mesosphere is 2–3 km and more. For instance, data of CRISTA-MAHRSI that will be considered in Sect. 4 have resolution dz~2 km. From the said above it follows that it is impossible to use the mathematically correct description of vertical transport (see Eqs. 8–9) in application to

data of measurements because of uncertainty in the choice of $D_{zz}(z)$ and $w_z(z)$ as well as because of insufficient altitude resolution of experimental data. Consequently, we first regard vertical transport characteristics to be unknown and infer the corresponding terms in the MPCS BDM equations simultaneously with vertical distribution of H_2O concentration in the upper mesosphere. Second, we take these terms into account in a simplified form. More specifically, vertical transport is taken into consideration in the equation for O concentration only, and terms describing transport are represented in the form of an unknown but constant in time (not in altitude!) source (or sink) I_O of O molecules, whose physical meaning corresponds to the equation

$$I_O = < \frac{\partial}{\partial z} D_{zz} \frac{\partial}{\partial z} O - \frac{\partial}{\partial z}(w_z \times O) > \quad (13)$$

Here $<\ldots>$ denotes averaging on the time interval $[t_{in}, t_{end}]$. Note that this approach, as before, allows us to use the zero-dimensional model but now it is necessary to infer simultaneously two unknown parameters (H_2O and I_O). Therefore, the described procedure of retrieving H_2O concentration is modified. Now, at each iteration, we change not only the value of H_2O concentration (in accord with Eq. 12) but also the value of I_O whose iterative scheme is written in the form

$$I_O^{new} = I_O^{old}(1 + \beta \times (O^{end} - O^{dv})/O^{end}), \quad (14)$$

where β=const$\ll$1. Therefore, for finding H_2O concentration we have to minimize two errors:

$$S_1 = (HO_x^{end} - HO_x{}^{dv})^2/(HO_x^{end})^2 \text{ and } S_2 = (O^{end} - O^{dv})^2/(O^{end})^2 \quad (15)$$

Retrieval of H_2O concentration ceases automatically as soon as the values of both the quantities $S_{1,2}$ become less than 10^{-8}.

Note that the proposed procedure neglects the source (or sink)

$$I_{HO_x} = < \frac{\partial}{\partial z} D_{zz} \frac{\partial}{\partial z} HO_x - \frac{\partial}{\partial z}(w_z \times HO_x) > \quad (16)$$

ACPD
9, 5753–5783, 2009

of molecules of the family of odd hydrogen due to vertical transport. This approximation is forced: terms defining I_{HO_x} enter the right-hand side of the same differential Eq. (9) (for the concentration of HO_x) as the source I_{H_2O} of interest to us. Therefore, in the absence of objective information about distributions of D_{zz} and w_z and with insufficient vertical resolution of experimental data we cannot, in principle, retrieve these terms separately. Consequently, following the proposed procedure (for the interval of heights from 70–75 km to 90 km) we find instead of I_{H_2O} the sum $I_{H_2O}+I_{HO_x}$, which leads, generally speaking, to "overestimated" values of retrieved H_2O concentrations. Error caused by such overestimation is, evidently, determined by vertical distribution of the coefficient of vertical eddy diffusion and characteristic values of vertical velocity. To evaluate possible error, the procedure of retrieval of H_2O concentration was tested on numerous examples of vertical distributions of H_2O and D_{zz}, both model and typical for the conditions of the summer mesosphere in which the CRISTA-MAHRSI campaign was conducted. Both, $D_{zz}(z)$=const distributions and the inferred profiles of this parameter borrowed from the works by Danilov and Kalgin (1992), Hocking (1992), Lübken (1993, 1997) were used. The testing procedure was described in Sect. 2. Our research revealed that for $D_{zz}(z)\equiv 0$ and $w_{0,1,2}\equiv 0$ the retrieved profile of H_2O concentration reproduces almost perfectly (with error less than 1%) a "true" profile of H_2O concentration throughout the modeled range of heights. The least bit pronounced differences appear (first of all at altitudes higher than 80 km) at relatively large values of transport parameters: $D_{zz}(z)\geq 50\,m^2\,s^{-1}$ and $w_{0,1,2}\geq 1\,cm\,s^{-1}$. Essential error (>50%) in the retrieved profile of H_2O concentration (when we can say that the proposed method ceases to work) is observed at $D_{zz}(z)\geq(4\text{–}5)\times 10^2\,m^2\,s^{-1}$ and $w_{0,1,2}\geq(30\text{–}50)\,cm\,s^{-1}$. Note that these values of D_{zz} and $w_{0,1,2}$ are much too high for the summer period. Our analysis demonstrates that the retrieved distributions of H_2O concentration reproduce well initial model ("true") distributions, both qualitatively and quantitatively up to heights of 85–87 km, if we use the real values of transport parameters. This is illustrated, in particular, in Fig. 1 where we show initial model distribution of $H_2O(z)$ (black curve) with two pronounced maxima and three profiles of this pa-

ACPD
9, 5753–5783, 2009

rameter retrieved by different initial "experimental" data ($\{O_3^{in}(z)$, $OH^{in}(z)\}$ and $\{O_3^{end}(z)$, $OH^{end}(z)\}$). In all the three considered cases, "experimental" data were calculated from a complete MPCS model with the same preset distribution of $H_2O(z)$ (black line), but for different distributions of vertical transport parameters and for different instants of local time t_{in} and t_{end}. The first profile (red curve) was retrieved by data calculated for $D_{zz}(z)=10^2\,m^2\,s^{-1}$, $w_0=2\,cm\,s^{-1}$, $w_{1,2}=5\,cm\,s^{-1}$ and the time instants t_{in}=08:00 a.m. and t_{end}=02:00 p.m. The second profile (blue curve) was retrieved by data calculated for $D_{zz}(z)$ Lübken (1993) (the METAL campaign), $w_0=2\,cm\,s^{-1}$, $w_{1,2}=10\,cm\,s^{-1}$ and the instants of time t_{in}=06:00 a.m. and t_{end}=06:00 p.m. The third profile (violet curve) was retrieved by data calculated from Lübken (1993) (the NLC 91 campaign), $w_0=2\,cm\,s^{-1}$, $w_{1,2}=10\,cm\,s^{-1}$ for t_{in}=09:00 a.m. and t_{end}=01:00 p.m. One can see that all the three retrieved profiles reproduce satisfactorily model distribution of H_2O concentration.

We analyzed sensitivity of the retrieved distributions of H_2O concentration to uncertainty of the values of initial data of experiments (see Table 2) and found that in all the cases 1% uncertainty of the data leads to moderate fluctuations of H_2O concentrations that do not exceed 1–2%. Figure 2 illustrates results of retrieval of H_2O concentration under the condition that the initial data (both pairs of distributions $\{O_3^{in}(z)$, $OH^{in}(z)\}$ and $\{O_3^{end}(z)$, $OH^{end}(z)\}$) "were measured" with the error of 5%. The uncertainty of retrieved values of H_2O concentrations as a function of height arising in this case varied within the ~(7–12)% range.

It was mentioned in Sect. 2 that all the most essential reactions between O, $O(^1D)$, O_3, H, OH and HO_2 are summarized in Table 1. Some of the reactions that are not included in the table may also affect mesospheric distributions of the above constituents, the most significant of which are reactions with participation of even hydrogen compounds H_2O_2, H_2 and CH_4. We included them in the complete MPCS model so as to clarify how these reactions may influence accuracy of retrieval of H_2O concentration. The mesospheric concentrations of H_2 and CH_4 change with the characteristic times significantly exceeding one day. Therefore, they were taken into account in the frame-

ACPD
9, 5753–5783, 2009

work of the model as parameters with vertical distributions which are typical for the time and location of the CRISTA-MARHSI measurements. The characteristic time of variations of the mesospheric H_2O_2 concentration is less than one day. Hence, the model included an additional differential equation to calculate evolution of this variable. As in the previous cases, the complete MPCS model complemented in the above way was used to obtain initial "experimental" data ($\{O_3^{in}(z)$, $OH^{in}(z)\}$ and $\{O_3^{end}(z)$, $OH^{end}(z)\}$) which were used then to retrieve the H_2O concentration. Our analysis revealed that the neglect of reactions with participation of even hydrogen compounds H_2O_2, H_2 and CH_4 leads, within the framework of the proposed procedure, to absolute error in retrieved H_2O concentrations at heights lower than 70 km. Calculations showed that, at 50–70 km, this error does not exceed ~0.2–0.3 ppmv, with the average value of error being ~0.1 ppmv. Bearing in mind that H_2O concentration in this range of heights is 6–7 ppmv (see e.g., Seele and Hartogh, 1999; Hervig et al., 2003), we are in a position to conclude that the corresponding relative error does not exceed 5%. This result (a secondary role of even hydrogen compounds H_2O_2, H_2 and CH_4) may be elucidated on an example of the reaction $H_2+O(^1D)\rightarrow H+OH$ which is most "influential" among the omitted reactions. At the heights of 50–70 km, the concentration of H_2O exceeds the H_2 concentration by more than 3–4 times (Sonnemann et al., 2005), and the value of the constant of this reaction is less than half of the constant of the reaction $H_2O+O(^1D)\rightarrow 2OH$. As a result, the contribution of the reaction $H_2+O(^1D)\rightarrow H+OH$ to the common source of odd hydrogen at the heights of 50–70 km turns out to be considerably smaller than that of the sum of the reactions $H_2O+O(^1D)\rightarrow 2OH$ and $H_2O+h\nu\rightarrow H+OH$. Above 65–70 km, the concentration of $O(^1D)$ decreases significantly. Hence, at such heights, the reactions employing this component become insignificant compared with the reaction $H_2O+h\nu\rightarrow H+OH$.

ACPD
9, 5753–5783, 2009

4 Retrieval of $H_2O(z)$ from CRISTA-MAHRSI data

During the second satellite CRISTA-MAHRSI campaign on 8–16 August 1997, vertical distributions of temperature, air concentration and two chemical MPCS constituents (OH and O_3) were measured simultaneously (Grossmann et al., 2002; Conway et al., 2000). Available data on hydroxyl concentration were measured for daytime hours at latitudes and altitudes of 15° S–71° N and 40–90 km, respectively, by ozone concentration at 18° S–73° N, 50–94 km, and by air temperature and concentration at 74° S–74° N, 29–91 km. As was noted above, this information is sufficient for inferring, using the MPCS BDM algebraic equations, simultaneous vertical distributions of O, $O(^1D)$, H, and HO_2 concentrations in the mesosphere (50–87 km) in a wide range of latitudes, longitudes and local times, and for further retrieval of vertical distributions of H_2O. In Fig. 3 we give by way of example vertical distributions of H, HO_2, HO_x and O concentrations obtained from the CRISTA-MAHRSI data measured on 13 August 1997 at 60–63° N, 355–360° W at local time instants t_{in}=08:00 a.m. and t_{end}=03:00 p.m. Omitting detailed analysis we note that qualitatively the results presented in the figures agree quite well with the available concepts of vertical distribution of these constituents (e.g., Brasseur and Solomon, 1986; Takahashi et al., 1996; Sandor and Clancy, 1998; Gumbel et al., 1998). Figure 4 shows vertical distribution of water vapor concentration (heavy solid curve and dark circles) retrieved using the proposed technique and the distribution of dynamic variables of MPCS BDM given in Fig. 3. It is clear from this figure, in particular, that within the considered range of heights $H_2O(z)$ has two pronounced maxima at 73 km and 81 km. The second profile of H_2O depicted in Fig. 4 (heavy dashed curve and open rhombs) was obtained from the CRISTA-MAHRSI data measured on 13 August 1997 at 63–65° N, 225–230° W at local time instants t_{in}=07:12 a.m. and t_{end}=02:30 p.m. This profile, like the previous one, has a well pronounced maximum at 73 km. The "upper" maximum is evidently higher than in the first case. We cannot make more definite conclusions as the corresponding CRISTA-MAHRSI data at ~83 km are "truncated". Note that both the profiles in Fig. 4 correspond to close values of latitude.

ACPD
9, 5753–5783, 2009

Nevertheless, they have pronounced qualitative and quantitative differences, evidently because they are strongly spaced apart (by about 4000 km) in zonal direction. This conclusion is supported by the results of retrieval of H_2O concentration presented in Fig. 5 that correspond to the CRISTA-MAHRSI data measured on 15 August 1997 at 69–71° N, 60–65° W at t_{in}=08:00 a.m. and t_{end}=00:18 p.m. (heavy solid curve and dark circles) and 66–68° N, 141–148° W at t_{in}=08:12 a.m. and t_{end}=01:30 p.m. (heavy dashed curve and open rhombs). One can see that in this case two spaced apart profiles agree well up to 73–75 km, but above these heights appreciable qualitative difference (up to 40–50%) in the corresponding values of H_2O concentration is observed.

5 Discussion

Note that the presence of two maxima in the distribution of H_2O concentration at 73 and 81 km shown by the heavy solid curve and dark circles in Fig. 4 agrees well, both quantitatively and qualitatively, with results of direct measurements. For example, the distribution of H_2O concentration measured by HALOE at 60–70° N (see McHugh et al., 2003) has maxima at 75 and 83 km with values of about 7.5 ppmv. Hervig et al. (2003) reported distribution with the value of H_2O concentration in the upper maximum equal to ~8.5 ppmv. Appearance of the upper maximum may be attributed to redistribution of H_2O concentration as a result of processes of formation, sedimentation and evaporation of particles of mesospheric clouds in the summer time at mesopause heights (Summers et al., 2001; Von Zahn and Berger, 2003). A possible cause of the second maximum of H_2O concentration (at 73–75 km) may be heterogeneous reactions of H_2O molecule formation on the surface of meteorite dust hypothesized by Summers and Siskind (1999). However, Sonnemann et al. (2005) showed that no heterogeneous reactions are needed to produce the high water vapor peak at 70 km or higher.

At the same time, below about 65–70 km, our results (see Figs. 4–5) differ appreciably from data of direct measurements. One can see that values of H_2O concentration retrieved at these heights are about 2–4 ppmv, whereas according to the HALOE data

these values are of order 6–7 ppmv (e.g., Hervig et al., 2003). We believe there are two most probable reasons for this discrepancy:

1. It may be conjectured that real values of constants of photochemical reactions differ strongly from the values recommended by JPL which we use in our research. Summers et al. (2001) showed that OH concentrations measured within the framework of MAHRSI at 69–71° N in the 50–79 km range of heights proved to be appreciably less (up to 50–60% less) than those calculated by the photochemical model with allowance for the distribution of H_2O concentration from HALOE. According to Summers et al. (2001) the cause of this discrepancy is the overestimated (by 50%) standard JPL value of constant of the reaction $O+HO_2 \rightarrow O_2+OH$. Figure 6 demonstrates the distribution of H_2O concentration which we retrieved by the CRISTA-MAHRSI data same as in Fig. 4 (heavy solid curve and dark circles), but for the reaction constant $R(5)=0.5\times R(5)_{JPL}$. One can see that the change of the value of the reaction constant results in a moderate (by about 2–3 ppmv) increase in the H_2O concentration at 50–65 km, but is much more pronounced at the heights of the middle mesosphere, resulting, in particular, in a considerable (by about 7 ppmv) increase in the lower maximum of $H_2O(z)$. Thus, upon the whole we can state that a change in the constant of the reaction $O+HO_2 \rightarrow O_2+OH$ does not markedly reduce discrepancy with results of direct measurements of H_2O. Such an analysis was undertaken for other photochemical reactions listed in Table 1, but we failed to find reasonable changes of their constants that would enable us to increase (up to admissible level) characteristic values of H_2O concentration below 65–70 km without substantial growth of concentration of this constituent above these heights.

2. The used data of OH concentration measurements at the heights of 50–70 km may be underestimated. In other words, the discrepancy noted by Summers et al. (2001) between the model and measured concentrations of OH may be due to unrecorded error of MARHSI measurements. This possibility is pointed

to indirectly by data of simultaneous balloon-borne measurements of vertical distributions of OH, HO_2, O_3 and H_2O at 69° N made by means of FIRS-2 at the heights of 30–50 km (Jucks et al., 1998) the same year as the MARHSI campaign. Jucks et al. (1998) showed that the OH concentrations measured by FIRS-2 agree well with model calculations with reaction constants complying with the JPL recommendations. Besides, direct comparison of data at 44–50 km given by Jucks et al. (1998) with results of MARHSI measurements demonstrates that "satellite" concentrations of OH prove to be less than data of more accurate balloon-borne measurements (please see Fig. 7). Relative value of this difference $(OH_{FIRS} - OH_{MARHSI})/OH_{MARHSI})$ grows with increasing height and amounts to about 33% already at 50 km. Note also that the value of $OH_{FIRS} \approx 1.76 \times 10^7$ cm^{-3} at 50 km corresponds almost exactly to the model value of the OH concentration at the same height, which was calculated by Summers et al. (2001) using the photochemical model with account for the distribution of H_2O concentration from HALOE and, as opined by Summers et al. (2001), is overestimated. Thus, given underestimated MARHSI data, one can hypothesize that measurement error of OH concentration above 50 km reaches even higher values, which, in the final analysis, explains low values of H_2O concentration at 50–70 km shown in Figs. 4–5.

6 Conclusions

We propose an indirect method for retrieval of a number of significant minor gas constituents of the atmosphere. The technique is based on the use of models of atmospheric photochemical systems simplified in a special manner. It is applied to results of simultaneous satellite CRISTA-MAHRSI measurements of O_3 and OH concentrations aimed at retrieving vertical distributions of H_2O concentrations in the mesosphere. It should be noted that the method may be applied to other atmospheric photochemical systems in troposphere and stratosphere.

ACPD
9, 5753–5783, 2009

Acknowledgements. The authors thank D. Offermann, M. Kaufmann, O. Gusev, and M. H. Stevens for the CRISTA-MAHRSI data they made available to us. The work was done under support of the RFBR (projects 06-02-16568 and 09-05-01041) and of the Program of Fundamental Research of the RAS Department of Physical Sciences "Physics of the Atmosphere: Electric Processes, Radiophysical Methods of Researches" (project 2.1).

References

Brasseur, G. and Solomon, S.: Aeronomy of the Middle Atmosphere, D. Reidel Publishing Company, Norwell, Mass., USA, 452 pp., 1986.

Conway, R. R., Summers, M. E., Stevens, M. H., Cardon, J. G., Preusse, P., and Offermann, D.: Satellite observations of upper stratospheric and mesospheric OH: The HO_x dilemma, Geophys. Res. Lett., 27, 2613–2616, 2000.

Crutzen, P. J., Grooß, J.-U., Brühl, C., Müller, R., and Russel III, R. J. M.: A reevaluation of the ozone budget with HALOE UARS data: No evidence of the ozone deficit, Science, 268, 705–708, 1995.

Danilov, A. D. and Kalgin, U. A.: Seasonal and latitudinal variations of eddy diffusion-coefficient in the mesosphere and lower thermosphere, J. Atmos. Terr. Phys., 54, 1481–1489, 1992.

Feigin, A. M. and Konovalov, I. B.: On the possibility of complicated dynamic behaviour of atmospheric photochemical systems: Instability of the Antarctic photochemistry during the ozone hole formation, J. Geophys. Res., 101(D), 26023–26038, 1996.

Feigin, A. M., Konovalov, I. B., and Molkov, Y. I.: Towards understanding nonlinear nature of atmospheric photochemistry: Essential dynamic model of the mesospheric photochemical system, J. Geophys. Res., 103, 25447–25460, 1998.

Fichtelmann, B. and Sonnemann, G.: On the variation of ozone in the upper mesosphere and lower thermosphere: a comparison between theory and observation, J. Meteorol., 39, 297–308, 1989.

Grossmann, K. U., Offermann, D., Gusev, O., Oberheide, J., Riese, M., and Spang, R.: The CRISTA-2 mission, J. Geophys. Res., 107, 8173, doi:10.1029/2001JD000667, 2002.

Gumbel, J., Murtagh, D. P., Espy, P. J., Witt, G., and Schmidlin, F. J.: Odd oxygen measurements during the Noctilucent Cloud 93 rocket campaign, J. Geophys. Res., 103, 23399–23414, 1998.

Hedin, A. E.: Extension of the MSIS thermospheric model into the middle and lower atmosphere, J. Geophys. Res., 96, 1159–1172, 1991.
Hervig, M., McHugh, M., and Summers, M. E.: Water vapor enhancement in the polar summer mesosphere and its relationship to polar mesospheric clouds, Geophys. Res. Lett., 30, 2041, doi:10.1029/2003GL018089, 2003.
Hocking, W. K.: Turbulence in the region 80–120 km, Adv. Space Res., 50, 153–161, 1990.
Jucks, K. W., Johnson, D. G., Chance, K. V., Traub, W. A., Margitan, J. J., Osterman, G. B., Salawitch, R. J., and Sasano, Y.: Observations of OH, HO_2, H_2O, and O_3 in the upper stratosphere: implications for HO_x photochemistry, Geophys. Res. Lett., 25, 3935–3938, 1998.
Körner, U. and Sonnemann, G. R.: Global three-dimensional modeling of the water vapor concentration of the mesosphere-mesopause region and implications with respect to the noctilucent cloud region, J. Geophys. Res., 106, 9639–9651, 2001.
Lübken, F. J.: Experimental results on the role of turbulence for the heat budget of the upper atmosphere, Habilitation Thesis, 160 pp., Bonn University, Germany, 1993.
Lübken, F. J.: Seasonal variation of turbulent energy dissipation rates at high latitudes as determined by in situ measurements of neutral density fluctuations, J. Geophys. Res., 102, 13441–13456, 1997.
Sander, S. P., Finlayson-Pitts, B. J., Friedl, R. R., Golden, D. M., Huie, R. E., Keller-Rudek, H., Kolb, C. E., Kurylo, M. J., Molina, M. J., Moortgat, G. K., Orkin, V. L., Ravishankara, A. R., and Wine, P. W.: Chemical Kinetics and Photochemical Data for Use in Atmospheric Studies, Evaluation Number 15, JPL Publication 06-2, Jet Propulsion Laboratory, Pasadena, p. 523, 2006.
Sandor, B. J. and Clancy, R. T.: Mesospheric HOx chemistry from diurnal microwave observations of HO_2, O_3, and H_2O, J. Geophys. Res., 103, 13337–13351, 1998.
Seele, C. and Hartogh, P.: Water vapor of the polar middle atmosphere: Annual variation and summer mesosphere conditions as observed by ground-based microwave spectroscopy, Geophys. Res. Lett., 26, 1517–1520, 1999.
Singer, W., Bremer, J., Hocking, W. K., Weiss, J., Latteck, R., and Zecha, M.: Temperature and wind tides around the summer mesopause at middle and Arctic latitudes, Adv. Space Res., 31(9), 2055–2060, 2003.
Sonnemann, G. and Fichtelmann, B.: Subharmonics, cascades of period of doubling and chaotic behavior of photochemistry of the mesopause region, J. Geophys. Res., 101, 1193–

1203, 1997.
Sonnemann, G., Kremp, C., Ebel, A., and Berger, U.: A three-dimensional dynamic model of the minor constituents of the mesosphere, Atmos. Environ., 32, 3157–3172, 1998.
Sonnemann, G. R., Grygalashvyly, M., and Berger, U.: Autocatalytic water vapor production as a source of large mixing ratios within the middle to upper mesosphere, J. Geophys. Res., 110, D15303, doi:10.1029/2004JD005593, 2005.
Summers, M. E., Conway, R. R., Siskind, D. E., Stevens, M. H., Offermann, D., Riese, M., Preusse, P., Strobel, D. F., and Russell, J. M.: Implications of satellite OH observations for middle atmospheric H_2O and ozone, Science, 277, 1967–1970, 1997.
Summers, M. E. and Siskind, D. E.: Surface recombination of O and H_2 on meteoric dust as a source of mesospheric water vapor, Geophys. Res. Lett., 26, 1837–1840, 1999.
Summers, M. E., Conway, R. R., Englert, C. R., Siskind, D. E., Stevens, M. H., Russell, J. M., Gordley, L. L., and McHugh, M. J.: Discovery of a water vapor layer in the Arctic summer mesosphere: Implications for polar mesospheric clouds, Geophys. Res. Lett., 28, 3601–3604, 2001.
Takahashi, H., Melo, S. M. L., Clemesha, B. R., Simonich, D. M., Stegman, J., and Witt, G.: Atomic hydrogen and ozone concentrations derived from simultaneous lidar and rocket airglow measurements in the equatorial region, J. Geophys. Res., 101, 4033–4040, 1996.

Table 1. List of reactions.

(1) $O+OH+M \rightarrow HO_2+M$	(11) $O+O+M \rightarrow O_2+M$
(2) $H+HO_2 \rightarrow O_2+H_2$	(12) $O_3+H \rightarrow O_2+OH$
(3) $OH+HO_2 \rightarrow O_2+H_2O$	(13) $O_3+OH \rightarrow O_2+HO_2$
(4) $O+OH \rightarrow O_2+H$	(14) $H+HO_2 \rightarrow 2OH$
(5) $O+HO_2 \rightarrow O_2+OH$	(15) $OH+OH \rightarrow O+H_2O$
(6) $O_2+H+M \rightarrow HO_2+M$	(16) $O_3+h\nu \rightarrow O_2+O(^1D)$
(7) $H_2O+h\nu \rightarrow H+OH$	(17) $OH+H+M \rightarrow H_2O+M$
(8) $O_2+h\nu \rightarrow 2O$	(18) $H+HO_2 \rightarrow H_2O+O$
(9) $O+O_2+M \rightarrow O_3+M$	(19) $O(^1D)+M \rightarrow O+M$
(10) $O+O_3 \rightarrow 2O_2$	(20) $H_2O+O(^1D) \rightarrow 2OH$

M – molecule of air.

Table 2. Sensitivity (%) of retrieved values of H_2O concentration to 1% uncertainty of initial experimental data.

	O_3^{in}	OH^{in}	O_3^{end}	OH^{end}
H_2O	50–80 km: 0–0.1 80–87 km: 0.1–0.3	50–80 km: 0–0.05 80–87 km: 0.05–0.3	0–1	1.5–2

ACPD
9, 5753–5783, 2009

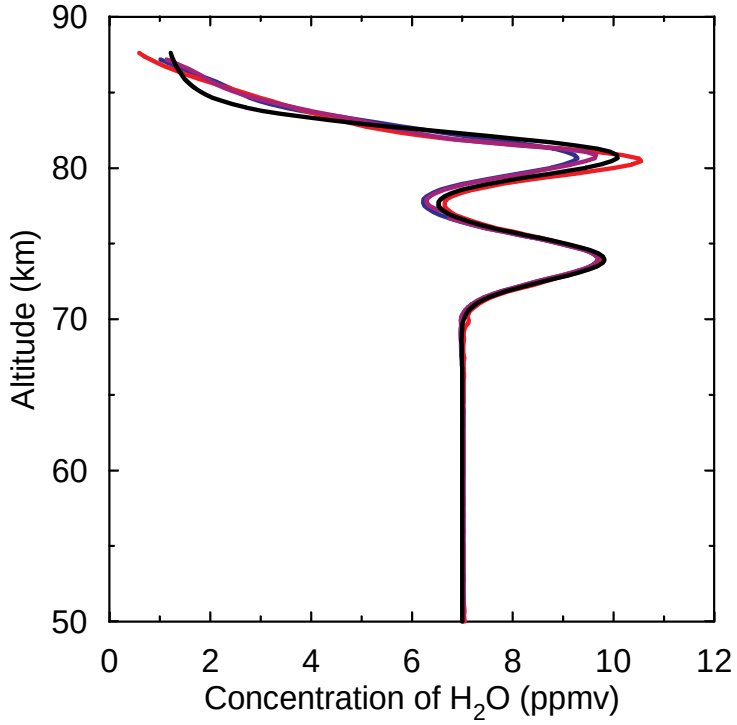

Fig. 1. Model (black curve) and retrieved (red, blue and violet curves) profiles of H_2O concentration (see the text for details).

ACPD

9, 5753–5783, 2009

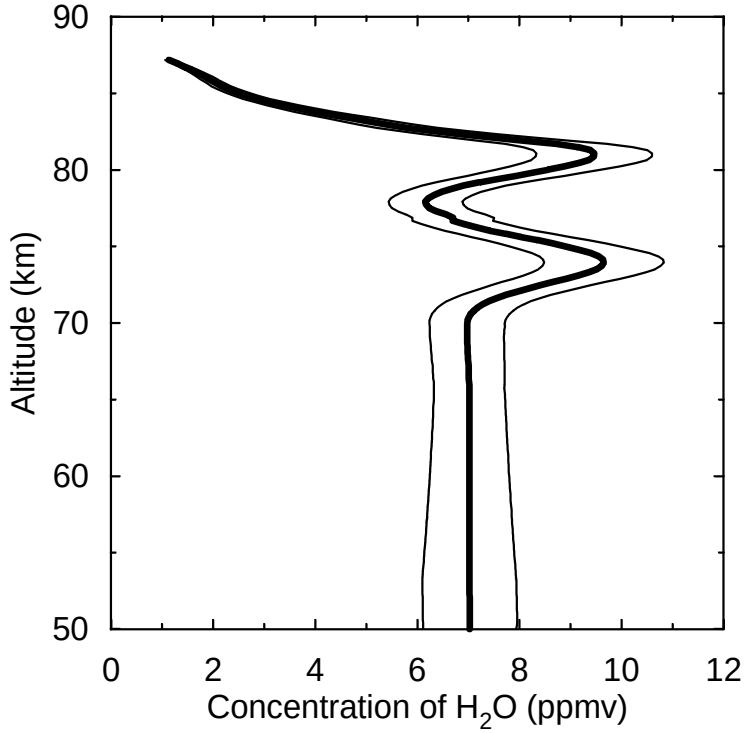

Fig. 2. The same as in Fig. 1 (violet curve), but with allowance for 5% uncertainty of initial data. The thin lines show uncertainty boundaries of retrieved values of H_2O concentration.

ACPD
9, 5753–5783, 2009

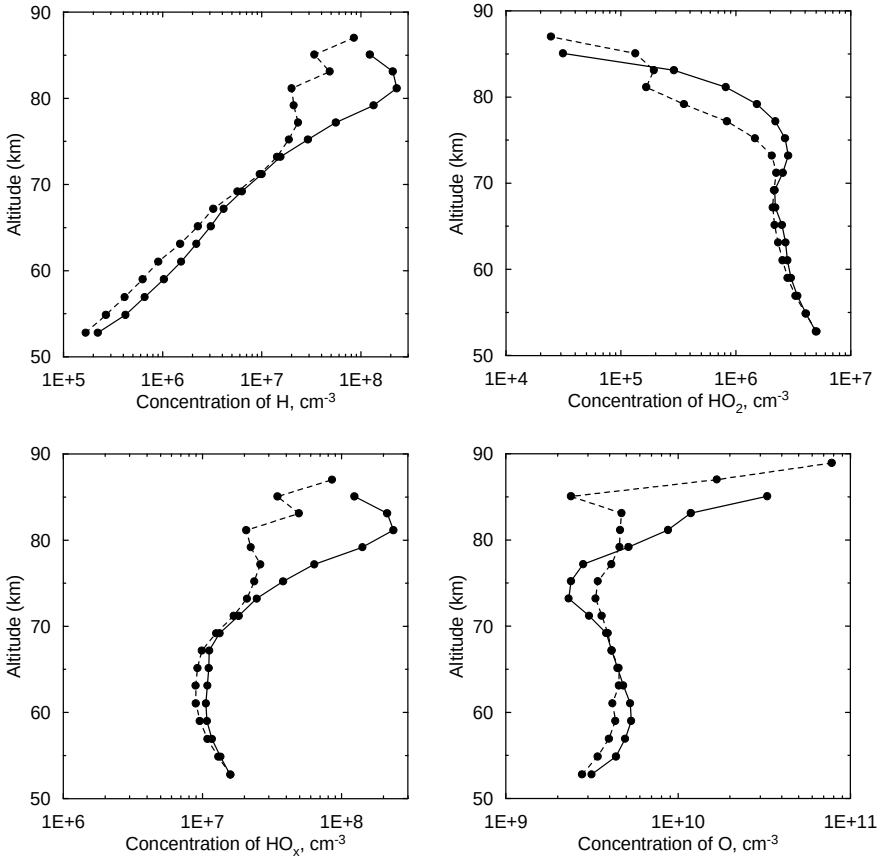

Fig. 3. Vertical distributions of H, HO_2, HO_x and O concentration at the instants of local time about 08:00 a.m. (dashed curve) and 03:00 p.m. (solid curve) retrieved from CRISTA-MAHRSI data measured on 13 August 1997 at 60–63° N, 355–360° W.

ACPD
9, 5753–5783, 2009

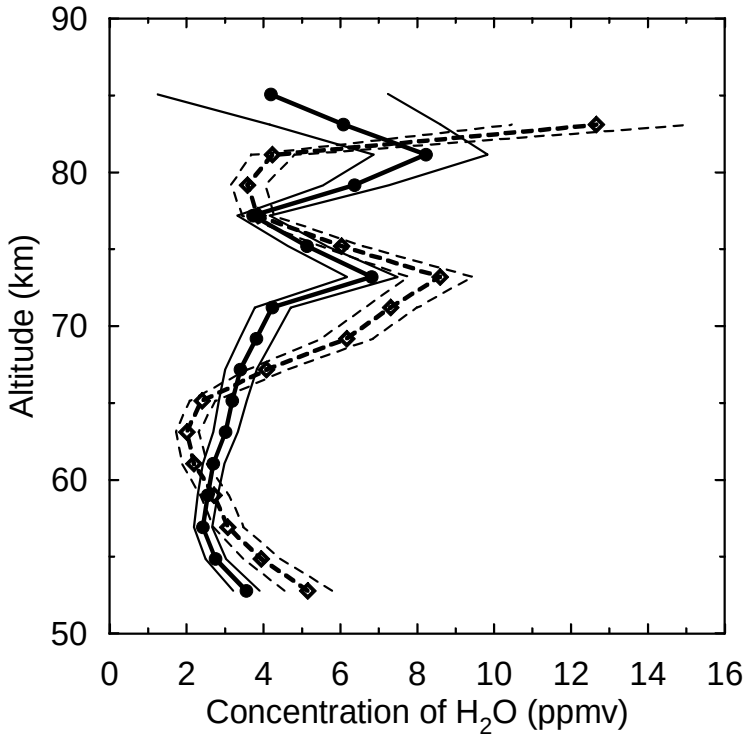

Fig. 4. Profiles of H_2O concentration retrieved from CRISTA-MAHRSI data measured on 13 August 1997 at 60–63° N, 355–360° W (heavy solid curve and dark circles) and 63–65° N, 225–230° W (heavy dashed curve and open rhombs). The thin curves show retrieval error corresponding to uncertainties of initial experimental data.

ACPD
9, 5753–5783, 2009

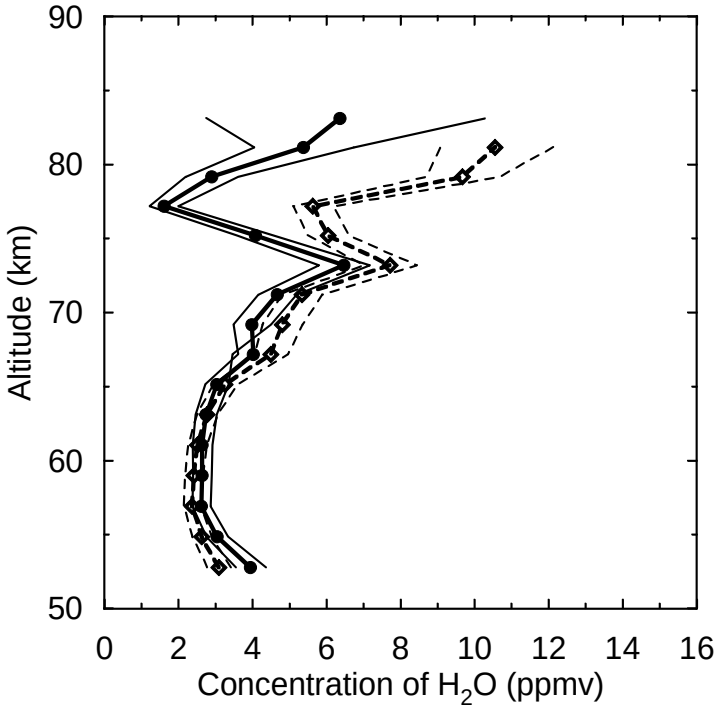

Fig. 5. Profiles of H_2O concentration retrieved from CRISTA-MAHRSI data measured on 15 August 1997 at 69–71° N, 60–65° W (heavy solid curve and dark circles) and 66–68° N, 141–148° W (heavy dashed curve and open rhombs). The thin curves show retrieval error corresponding to uncertainties of initial experimental data.

ACPD
9, 5753–5783, 2009

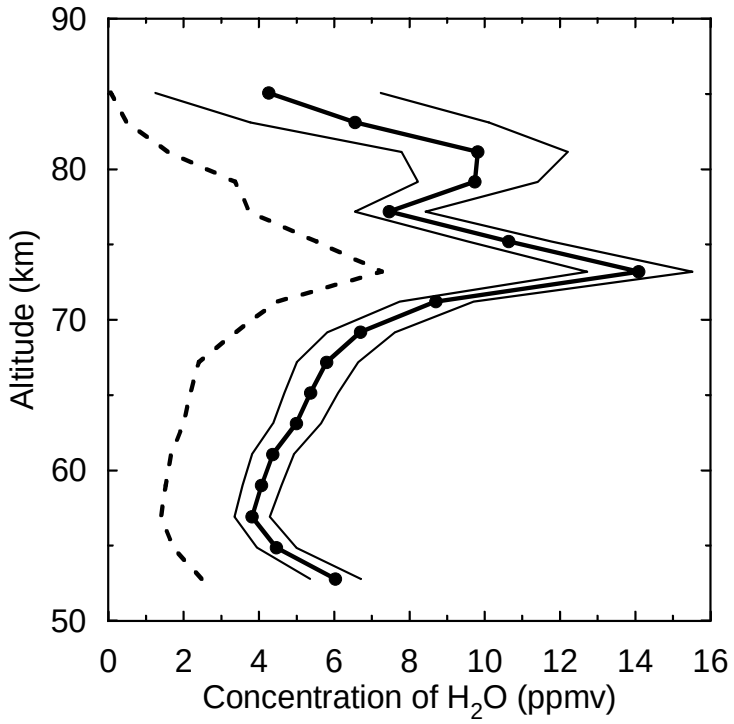

Fig. 6. The solid curves show vertical distribution of H_2O concentration retrieved from the same CRISTA-MAHRSI data as in Fig. 4 (heavy solid curve and dark circles), but for $O+HO_2 \rightarrow O_2+OH$ $R(5)=0.5\times R(5)_{JPL}$. The dashed curve shows an increase in H_2O concentration as a function of height as a result of decreasing reaction constant.

ACPD
9, 5753–5783, 2009

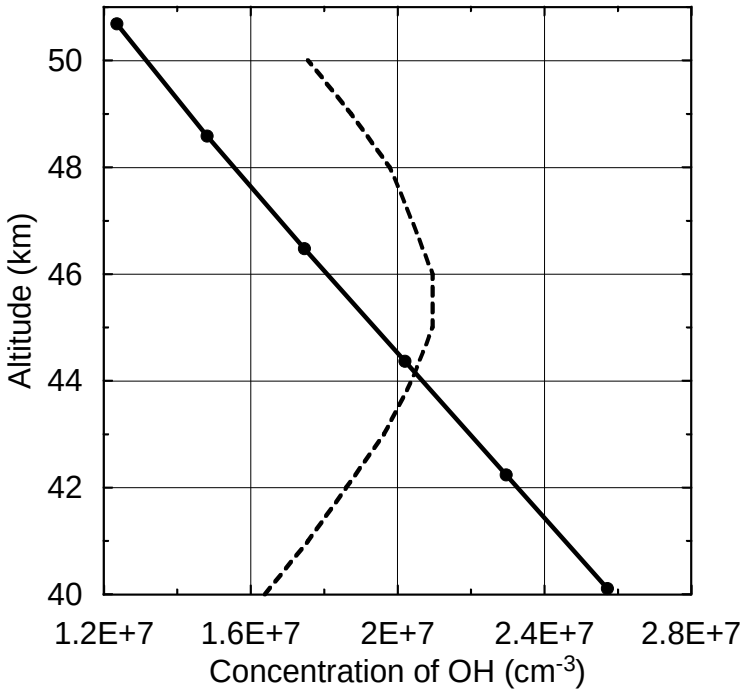

Fig. 7. The solid curve shows vertical distribution of OH concentration at 40–50 km averaged over eight profiles of OH concentration obtained in MAHRSI campaign, which were used to retrieve vertical distribution of H_2O concentration in Figs. 4 and 5. The dashed curve shows vertical distribution of OH concentration from Jucks et al. (1998) measured by FIRS-2 on 30 April 1997 at 69° N (see explanations in the text).

ACPD
9, 5753–5783, 2009